Journal of
Materials Chemistry C

REVIEW

View Article Online
View Journal | View Issue

Cite this: *J. Mater. Chem. C*, 2018, **6**, 11943

Received 19th July 2018,
Accepted 15th October 2018

DOI: 10.1039/c8tc03573c

rsc.li/materials-c

Ullazine-based materials: towards novel opportunities in organic electronics

Cristina Cebrián

Polycyclic aromatic hydrocarbons (PAHs) constitute a remarkable class of organic compounds that exhibit a large palette of electronic and optical properties. During the last decade, particular interest has been devoted to these PAHs driven by their successful application in organic electronics. Controlled heteroatom-doping of PAHs (Het-PAHs) offers additional possibilities for property modulation, rendering these derivatives very appealing for the development of high performing materials. In this article, we report a newly emerging class of materials based on a N-PAH class known as ullazine. Briefly covering different synthetic methodologies, their properties will be highlighted with special attention to their current fields of application, mostly in solar energy conversion, although there is great promise for this type of Het-PAH-based material.

1. Introduction

Traditionally viewed as chromophores, the development of heteroatom-doped polycyclic aromatic hydrocarbons (Het-PAHs) is attracting renewed attention due to their easily tunable properties in comparison with their parent PAH congeners.[1–3] Het-PAHs can be regarded as small cut-offs of heteroatom-containing graphene with a non-zero bandgap that endows them with semiconducting properties. Their properties are tuned by varying the number of rings and their geometrical arrangement.[4–8] More importantly, the fascination for Het-PAH stems from the additional possibilities of electronic structure modification attained by the controlled introduction of heteroatoms within the compounds, resulting in modified physicochemical, optical, electrochemical and structural properties.[1,2] Indeed, contrary to the doping of graphene layers,[9] the step-wise construction of these polycyclic systems containing well-defined heterocyclic units allows for a precise heteroatom doping at the atomic level, *i.e.* in heteroatom type, content and position.[1,2,7]

Another interesting feature of Het-PAHs is their extended sp^2-hybridized framework, which plays a pivotal role in molecular organization. The close interplay of the interactions among π-electronic clouds, dipole moments and heteroatom contacts, among others, results in a subtle control of the molecular organization, creating excellent scaffolds to obtain self-assembled materials.[10–14]

Up to now, nitrogen has been the most common doping element in PAH-based compounds (N-PAHs) since it allows for property modulation without disruption of the structure.[1,15–17] Interestingly, opposite effects can be attained depending on the nature of the N atom. For instance, pyridinic-type N atoms typically confer electron-accepting properties[18–21] while pyrrolic-type N atoms, on the contrary, lead to electron enriched compounds.[15,22] Furthermore, peripheral imines constitute donor coordination sites, opening the door to organometallic complexes with interesting electronic and photophysical properties.[23] As a result, N-PAH-based materials keep gathering considerable interest owing to their potential applications in molecular electronics.

Université de Lorraine, CNRS, L2CM 1 Boulevard François Arago – BP 95823, F-57000 Metz, France. E-mail: cristina.cebrian-avila@univ-lorraine.fr

Cristina Cebrián

Cristina Cebrián is an Assistant Professor at the University of Lorraine (France). She studied Chemistry at the University of Castilla-La Mancha (Spain), where she also received her PhD in 2011 under the supervision of Prof. A. Díaz-Ortiz and Dr P. Prieto. During her doctoral studies, she made short stays in the groups of Prof. F. P. Cossío (University of the Basque Country, Spain) and Prof. L. De Cola (University of Münster, Germany). After a post-doctoral fellowship in De Cola's group (2012–2013) between the University of Münster and the University of Strasbourg (Institut de Science et d'Ingénierie Supramoléculaires, France), she obtained her current position at the UL in 2013. Her research interests include the synthesis of organic and organometallic materials for optoelectronics and solar energy conversion, with special attention to sustainable synthetic approaches and challenging photoactive systems based on non-toxic and alternative metals.

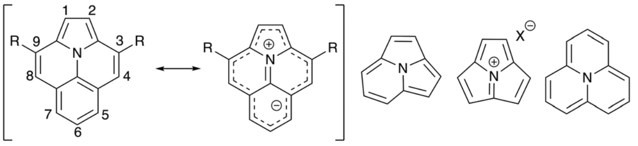

1a (R = H)
1b (R = Me)
1c (R = *t*-Bu)
1d (R = Ph)

2

3

4

Fig. 1 Some examples of the most representative cyclazines. In the case of ullazine **1**, its ionic mesomeric structure in which a [14]annulene is identified at the periphery is also provided.

In the last five years, the number of reports dealing with derivatives of indolizino[6,5,4,3-*ija*]quinoline, also known as ullazine, has experienced a sudden increase, having first been described in 1982 (compounds **1**, Fig. 1).[24] The successful application of ullazine-based photosensitizers in dye-sensitized solar cells (DSSCs) has subsequently fostered the development of new synthetic methods to obtain more sophisticated ullazine derivatives. Furthermore, in-depth characterisation studies of these novel materials are just beginning to shed light on alternative applications. Thus, we will herein present these very recent results, firstly briefly describing the basic features of the ullazine system. Then, an overview of the current available synthetic designs will be given as well. The following sections will be devoted to (potential) fields of application for ullazine-based materials, such as photosensitizers for solar cells (Section 3), charge-transporting materials for organic field-effect transistors (Section 4) and open-shell systems (Section 5). Finally, we will discuss the future outlook of this class of N-doped materials.

2. Ullazines: features and synthesis

Ullazine derivatives belong to the family of the cyclazines. This term was initially proposed by Boekelheide *et al.* when they reported the synthesis of pyrrolo[2,1,5-*cd*]indolizine (**2**) in 1958. Interestingly, this compound possesses a 10 π-electron conjugated system in the periphery, which confers it with aromatic character. They proposed the word cyclazine to generally designate "a conjugated, unsaturated cycle held planar by three covalent bonds to an internal nitrogen atom".[25] In Fig. 1, some of the most representative examples of cyclazines are depicted. It is worth noting that this class of compounds constitutes an elegant manner to achieve planar annulenes of different sizes upon bridging the conjugated system by the central N atom. As a result, cyclazines can present either aromatic or antiaromatic character and have acted as models to fully understand aromaticity.

From an electronic point of view, ullazine is isoelectronic with pyrene. However, in contrast to the apolar nature of the latter, ullazine presents a noticeable participation of an ionic mesomeric structure in the ground-state electronic description (Fig. 1). Indeed, an aromatic [14]annulene can be identified in the periphery for the ionic structure, justifying its important weight in the molecular description of the ground state.[24] Therefore, ullazine can be regarded as an intramolecular donor–acceptor system, which is at the origin of the particular appeal of ullazine derivatives.

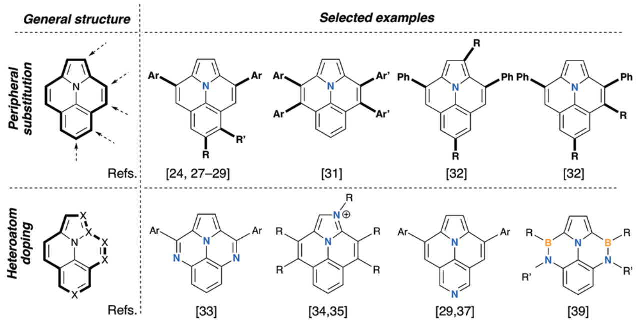

Fig. 2 Overview of selected functionalizations and heteroatom-doping reported for the ullazine core.

Furthermore, oxidation is readily observed for this Het-PAH due to its electron-donor nature conferred by the pyrrolic moiety. Interestingly, Gerson and Metzger found that the obtained radical cations for ullazines **1a–d** were persistent, even for several days.[26] Even more surprising was the fact that these compounds led also to radical anions with a non-negligible persistence.[26]

2.1 Accessible ullazine molecular designs

Following the recent synthetic interest for ullazine derivatives, multiple strategies for structural modification are currently available (Fig. 2). In almost all cases, the synthesis of the ullazine scaffold can be achieved starting from *N*-phenylpyrroles and, as a function of the selected method, different substitution patterns can be obtained.[24,27–32] Moreover, post-functionalization is also possible.[27,30] The electron-rich character of the ullazine system makes it prone to react with electrophilic reagents, position 5 being mostly favoured. Thus, the structural versatility attained so far in the synthesis of ullazine derivatives has turned it into a valuable building block for material fabrication.

The presence of additional heteroatoms has also been reported. As shown in Fig. 2, additional pyridinic-like nitrogen atoms can be incorporated at variable positions on the molecular periphery.[29,33–38] Even a bis-BN ullazine has been reported very recently,[39] with BN-doped PAH possessing high interest in organic

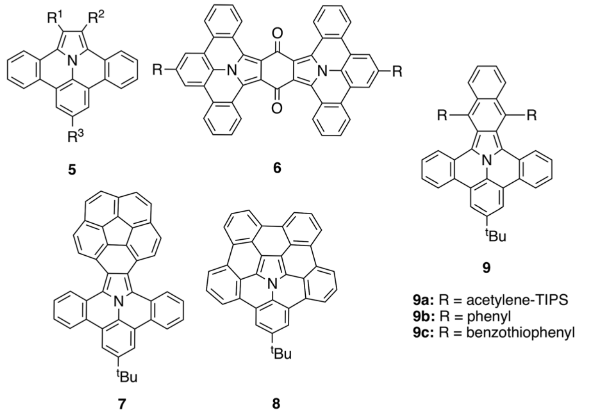

Fig. 3 Selected examples of π-extended conjugated systems based on the ullazine moiety.

electronics because of the introduction of polarity without disruption of the carbon framework.[40–43]

Additionally, ullazine derivatives with π-extended conjugated systems have been described as well (Fig. 3).[14,44–48] Notably, the 1,3-dipolar cycloaddition independently developed by the groups of Feng and Müllen[45,46] and that of Ito and Nozaki[14,47,48] is of particular importance for the easy access to large Het-PAHs such as **5–9**.

3. Ullazine-based photosensitizers for solar cells

Regardless of their organometallic or metal-free nature, DSSC photosensitizers generally comprise a donor–π–acceptor (D–π–A) structure.[49,50] Among the advantages of this configuration, the presence of low-energy charge-transfer (CT) electronic transitions is of utmost importance.[51] Indeed, the charge separation induced upon photoexcitation of the molecule greatly favours the subsequent electron injection into the semiconductor (SC) conduction band (CB) if corresponding electronic energy levels are properly placed.[50] Particularly for all-organic dyes, D–π–A designs also lead to bathochromically shifted absorptions in comparison to localized transitions, further improving solar light harvesting.[51]

To date, ullazine structural motifs have mostly been used for the engineering of novel photosensitizers for solar-cell fabrication purposes. The prominent electron-rich character of these derivatives can be exploited as the donor component. Nevertheless, as previously stated, the presence of the internal pyrrolic nitrogen within the conjugated framework promotes an intramolecular CT (ICT) resonance structure, intrinsically constituting both the donor and acceptor counterparts.

Delcamp, Grätzel and co-workers first reported ullazine-based sensitizers for DSSCs.[27] After a straightforward, easily scalable synthesis of the ullazine core, grafting groups were introduced at different positions, namely 5 (**JD21**, **JD25**, **JD29** and **JD30**), 4 (**JD26**) and 6 (**JD32**) (Fig. 4a). Thus, six novel dyes were obtained with varying donors and π-spacers. Most compounds exhibited an ICT absorption band almost extending throughout the whole visible spectrum. The presence of either alkoxy or triarylamine groups increased the molar absorptivity values (2.8, 3.3 and 2.4 × 10^4 M^{-1} cm^{-1} for **JD21**, **JD25** and **JD29**, respectively) with respect to alkyl-substituted **JD30** (1.2 × 10^4 M^{-1} cm^{-1}). Introduction of the cyanoacrylic anchoring group at the 4-position leads, however, to a noticeable decrease of the ICT absorption in comparison to the 5-substituted dyes. This result was attributed to the reduced planarity of the so-obtained chromophore, which was nicely supported by computational calculations. In the case of **JD32**, the ullazine core was modified at the 6-position, adding both the cyanoacrylic moiety and a thiophene ring as π-spacer. Nevertheless, the presence of a nodal plane at the frontier molecular orbitals (MOs) results in almost negligible electronic communication between the ullazine core and the acceptor unit. As a consequence, no distinguishable ICT band was discerned for **JD32**. Suitable redox properties prompted their evaluation within a DSSC scheme. Except for **JD32**, all dyes showed a broad incident photon-to-electron conversion efficiency (IPCE) covering from the UV to the red part of the spectrum, with peak values of *ca.* 70–95% (Fig. 4b). The broadened IPCE bands compared to the solution-state absorption revealed the presence of dye aggregation within the device. As expected, the introduction of flexible chains had a positive effect on the V_{oc} due to the protecting effect of the semiconductor surface towards electronic recombination with electrolyte. Dye **JD21** showed the best performance, attaining a remarkable power conversion efficiency (PCE) of 8.4% together with a short-circuit current density (J_{sc}) of 15.4 mA cm^{-2}, an open-circuit voltage (V_{oc}) of 730 mV and fill factor (FF) of 0.75.

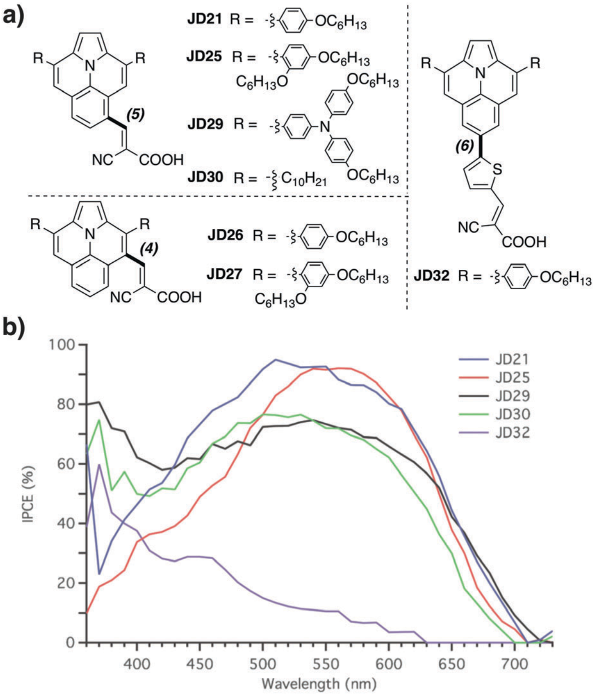

Fig. 4 (a) Molecular structures of ullazine-based dyes **JD21**, **JD25–27**, **JD29**, **JD30** and **JD32**. (b) Associated IPCE spectra of DSSC devices containing these dyes. (b) reprinted with permission from ref. 27 (Copyright © 2013 Wiley-VCH Verlag GmbH & Co. KGaA, Weinheim).

In spite of the good efficiencies achieved, several problems are associated with the widely employed liquid electrolytes within this type of photovoltaic device. Among them, leakage, evaporation of the solvent, flammability and corrosion issues are the most significant.[50] Therefore, the development of solid-state electrolytes such as p-type semiconducting polymers has progressively gained great interest. In this context, the promising results obtained with ullazine-based dyes encouraged the same authors to test their 5- and 4-substituted photosensitizers (**JD21**, **JD25–27**, **JD29** and **JD30**) in a solid-state DSSC (ssDSSC) selecting 2,2′,7,7′-tetrakis(*N*,*N*-di-*p*-methoxyphenylamine)-9,9′-spirobifluorene (spiro-MeOTAD) as the hole transporting material (HTM).[52] Compared to their solution spectra, the absorption spectra of the dyes adsorbed onto TiO_2 exhibited modified features, with different ICT band shapes and hypsochromically-shifted maxima. These results revealed dye loading as a critical parameter for the final device performance. In this regard, compound **JD29** bearing triphenylamine-type donors afforded the highest dye coverage. But, except for **JD29**, the dye coverage values reflected the steric hindrance exerted by the flexible alkyl/alkoxy chains well. In this regard, less encumbered dyes such as **JD21** or **JD30** were adsorbed to a higher extent. Evaluation of the photovoltaic performance of the fabricated ssDSSCs gave efficiencies in the range of 2.11–4.95%, with **JD29** giving the best results. The good performance of **JD29** was mainly attributed to its high V_{oc} as a result of the good dye coverage. Indeed, recombination rates between TiO_2 and spiro-MeOTAD were minimized together with an upward shift of the CB probably obtained as the result of a dipole moment effect exerted by adsorbed molecules. Additional improvement of these devices was achieved by fabricating a co-sensitized ssDSSC by using both **JD29** and **D35**[53] dyes, the latter allowing a better light harvesting, thus obtaining an increased PCE of 5.40%.

Tan and co-workers synthesized a new series of photosensitizers based on a 5-substituted ullazine core with the incorporation of different π-spacers and acceptor units (Fig. 5).[54] According to their study, the impact of the anchoring group is clearly more pronounced. In fact, compound **QD1** that possesses a cyanoacrylic acid led to a bathochromically shifted ICT band when compared to **QD2** and **QD3**, which respectively had phenylethylene and thiophene ethylene π-spacers along with carboxylic acid as the anchoring group. Impressive differences in the behaviour of **QD1** with respect to **QD2–QD3** were observed during device operation. **QD1** yielded a peak IPCE value of 80% at 520 nm while values of 20% at 466 nm and 19% at 464 nm were achieved by **QD2** and **QD3**, respectively. The higher efficiency of **QD1** was ascribed to a notable J_{sc} value of 12.28 mA cm^{-2} arising from better charge generation and transport.

A different approach was proposed by Mathew and co-workers (Fig. 6a).[55] These authors combined this unit with an ullazine moiety as a donor group, thus synthesizing the ullazine–porphyrin dyad **SM63**. Evaluation of the effect of the ullazine donor group was done by selecting a reference compound, namely **LD14-C8**,[56] which possessed a 4-dimethylaminophenyl group instead. Prominent modification of the optical properties was observed for **SM63**. The Soret band appeared to be drastically deformed into two bands with the Q-band being shifted towards lower energies. As confirmed by cyclic voltammetry, these changes were explained by an effective increase in the electronic conjugation in the dyad **SM63**. However, the lower symmetry of **SM63** as well as a slightly bent structure with respect to **LD14-C8** led to a concomitant reduction of the molar absorptivity of the Soret band. DSSCs with double layer TiO_2 photoanodes fabricated for both dyes generated efficiencies of 7.35 ± 0.13% (J_{sc} = 14.43 ± 0.27 mA cm^{-2}, V_{oc} = 0.70 ± 0.01 V, and FF = 0.73 ± 0.01) and 8.45 ± 0.16% (J_{sc} = 15.72 ± 0.26 mA cm^{-2}, V_{oc} = 0.73 ± 0.02 V, and FF = 0.74 ± 0.01) for **SM63** and **LD14-C8**, respectively (Fig. 6b and c). **SM63** particularly suffered from aggregation, which was partially controlled by addition of chenodeoxycholic acid (CDCA) and the use of less polar adsorption solvents. But, the still non-negligible degree of aggregation resulted in detrimental quenching of excited states and, ultimately, in lower J_{sc} values. Nevertheless, the larger harvesting of green (550 nm) and red (>700 nm) light undoubtedly demonstrates the great potential of the strong donor ullazine moiety for the development of panchromatic sensitizers.

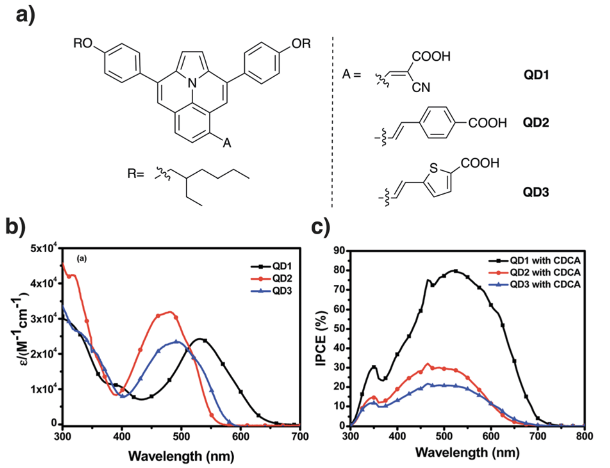

Fig. 5 (a) Molecular structures for the series of dyes **QD1–3** containing ullazine as the donor moiety and different π-spacers and anchoring groups. (b) Absorption spectra of **QD1–3** in 10^{-5} M $CHCl_3$. (c) Photocurrent action spectra for DSSC devices using **QD1–3** as dyes. (b) and (c) reprinted with permission from ref. 54 from The Royal Society of Chemistry.

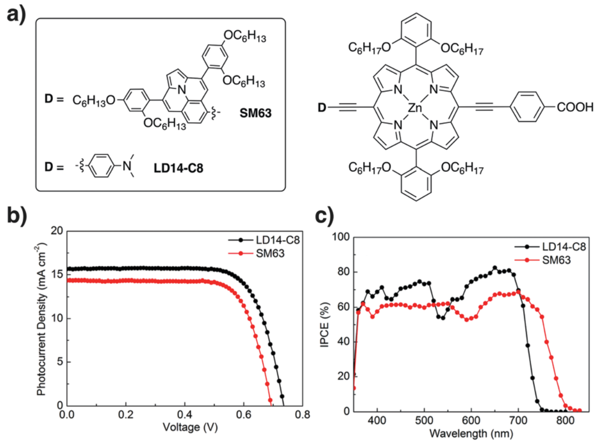

Fig. 6 (a) Molecular structures of **SM63** and **LD14-C8** photosensitizers. (b) *J–V* averaged characteristics for 3 cells sensitized with **LD14-C8** (black) and **SM63** (red) under AM 1.5G illumination (1000 W m^{-2}). (c) Associated IPCE spectra of DSSCs containing **LD14-C8** (black) and **SM63** (red) as dyes. Figures b and c reproduced from ref. 55 with permission from The Royal Society of Chemistry.

As previously stated, typical modification of ullazine derivatives *via* aromatic electrophilic substitutions takes place preferentially at the 5-position and, to a lesser extent, at the 4-position. In order to properly address the effects of the acceptor placement at the ullazine scaffold, Nazeeruddin and co-workers reported very recently a simple, elegant and selective synthesis of different regioisomers, 2-, 4-, 5- and 6-substituted ullazine-containing D–A sensitizers.[32] The localisation of the dihexylmalonate acceptor moiety had a distinct impact on the opto-electronic properties of the dyes. All derivatives showed similar electronic absorption features, *i.e.* two sets of bands. Those appearing at high energies corresponded to π → π* transitions, while the nature of the lower-energy ones would be better ascribed to an admixture of both π → π* and ICT. The relative percentage of the CT component varied according to the substitution. Ullazine D–A dyes with the acceptor moiety at the 4- and 6-position showed narrower, structured bands in the 350–425 nm region. In contrast, broader and less structured bands were observed for those 2- and 5-substituted, being bathochromically shifted as well. The trend for the CT efficiency can be established as follows: 5- > 2- > 4- > 6-substitution. In consequence, the 5-substituted compound possessing the larger ICT component was subsequently embodied in a perovskite solar cell as a dopant-free HTM. The best devices exhibited a modest PCE value of 13.08% (J_{sc} = 18.47 mA cm^{-2}, V_{oc} = 1.054 V, and FF = 0.671) for this kind of photovoltaic device. Nevertheless, the here-described protocols do allow the easy synthesis of tailor-made ullazine-based photosensitizers, giving access to a fine-tuning of their properties, which turns them into appealing materials for organic electronics.

4. Charge-transport properties of ullazine derivatives for OFETs

Due to their semiconducting properties, (Het-)PAHs are ideal candidates for the fabrication of organic field-effect transistors (OFETs).[57–63] Continuous research in this field is motivated by the application of this technology in the development of flexible displays,[64] stretchable devices,[65] sensors,[66] electronic paper,[67] and so forth. To date, there is a large number of p-type semiconductors based on small molecules and polymers, with charge mobilities well comparable to that of polycrystalline silicon.[68] However, their n-type counterparts have been less developed, exhibiting lower charge mobilities and poor device stabilities in air.[59,69]

Among the different synthetic strategies for the preparation of suitable n-channel materials, the introduction of electron-withdrawing groups is widely employed. In this regard, Klauk, Müllen, Li and co-workers have very recently described the synthesis of a set of carbonyl-/dicyanomethylene-functionalized π-extended ullazines **10–12** (Fig. 7a).[70] These compounds nicely exhibited two reversible reduction waves that can be ascribed to either the carbonyl group or the dicyanomethylene moiety. One oxidation wave was also observed, which was attributed to the central nitrogen atom. Estimated LUMO energies from the electrochemical data were of *ca.* −4 eV, which prompted the authors to test the performance of bis(dicyanomethylene)-substituted **12a** and **12b** as *n*-semiconductors in thin-film transistors (TFTs). Following a bottom-gate, top-contact architecture, the fabricated devices gave electron mobilities up to 0.02 and 0.06 cm^2 (V s)$^{-1}$ for compounds **12a** (Fig. 7b and c) and **12b** (Fig. 7d and e), respectively. Performance after 30 months in air was satisfactory for compound **12a**, still attaining an electron mobility of 0.006 cm^2 (V s)$^{-1}$, while the device embedding compound **12b** proved to be genuinely stable. Alternatively, the introduction of both carbonyl and dicyanomethylene groups had a clear auxochromic effect, reaching molar absorptivity values of 80 000 M^{-1} cm^{-1} for orange-red absorbing **12**. As a result, this new family of functionalized π-extended ullazines **10–12** showed appealing properties as both n-type semiconductors and colorants.

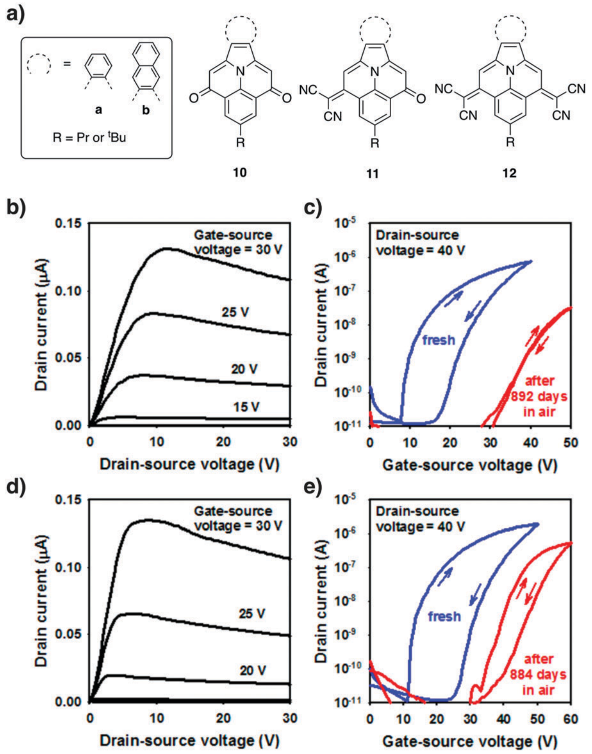

Fig. 7 (a) Carbonyl-/dicyanomethylene-functionalized π-extended ullazines **10–12**. *I–V* plots of n-channel thin-film transistors (TFTs) containing vacuum-deposited layers (30 nm) of **12a** (b, c) and **12b** (d, e). (b–e) reprinted with permission from ref. 70. Copyright 2018 American Chemical Society.

5. Stable open-shell ullazines

Control over the frontier orbital energy levels allows a precise modulation of the electronic and photophysical properties of any material, playing a key role in practical applications. Among the different synthetic approaches, extension of the π-conjugated system is an efficient common strategy.[71–74] In this regard, construction of (Het-)PAHs provides an excellent platform for property fine-tuning, along with appealing features for supramolecular arrangements.[1–3,7]

Unfortunately, handling of large (Het-)PAHs becomes very difficult due to solubility and stability issues. As for the stability, on increasing the size of this type of systems, the relative energy between closed-shell (CS) and open-shell (OS) electronic configurations is reduced, resulting in more eminent di(multi)radical character.[75–77] Nevertheless, these features have been receiving a great deal of attention for the last few decades owing to potential applications in organic electronics, spintronics, nonlinear optics and energy storage.[78–83] Phenalenyl radical is the smallest PAH exhibiting a persistent OS. Embedding this moiety into larger structures constitutes a

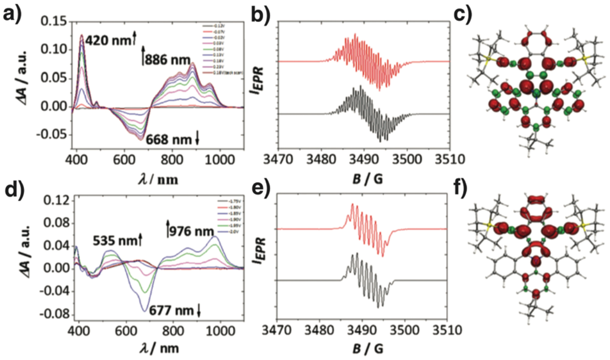

Fig. 8 (a) *In situ* differential UV-vis spectra of **9a** upon oxidation. (b) EPR signals of **9a**$^{\bullet+}$ (black: experimental and red: calculated). (c) DFT-computed spin density distribution in **9a**$^{\bullet+}$. (d) *In situ* differential UV-vis spectra upon reduction of **9a**. (e) EPR signal of **9a**$^{\bullet-}$ (black: experimental and red: calculated). (f) DFT-computed spin density distribution in **9a**$^{\bullet+}$. Reproduced from ref. 86 with permission from The Royal Society of Chemistry.

common strategy to obtain original OS materials.[80,84] Moreover, addition of heteroatoms such as O[85] or N,[45,77] jointly with extended π-conjugated structures and/or bulky substituents,[79,80] contributes to the stabilisation of the radical species. Very recently, Berger, Feng and co-workers investigated the electronic ground state ullazine derivatives **9a–c** whose core resulted from the combination of 9a-azaphenalene and perpendicularly-oriented naphthalene (Fig. 3).[86] All three compounds presented different conformers in solution, presenting a preponderant CS singlet ground state with a weak diradical character for some geometries. These π-extended ullazines showed appealing optical features, presenting broadband absorption covering the large part of the visible spectrum and emission in the red region. It is worth mentioning the facile generation of radical cation species upon oxidation with $AgSbF_6$, preparing **9a**$^{\bullet+}$, **9b**$^{\bullet+}$ and **9c**$^{\bullet+}$ (with SbF_6^- as counteranion) in 84%, 79% and 71% yield, respectively. Close inspection of the oxidation process was undertaken by UV-vis absorption and *in situ* spectroelectrochemistry. Generation of radical cations led to the appearance of a bathochromically shifted band into the near infrared part of the spectrum (Fig. 8a, *e.g.* **9a**$^{\bullet+}$ formation). Interestingly, additional characterisation using *in situ* electron paramagnetic resonance showed a broad signal for both **9a**$^{\bullet+}$ (Fig. 8b) and **9c**$^{\bullet+}$, with a hyperfine structure and a *g*-factor of 2.0025 and 2.0024, respectively. DFT calculations revealed that the spin density is localized over the full π-core (Fig. 8c). As for **9a**, generation of the radical anion **9a**$^{\bullet-}$ (broad signal with hyperfine structure, *g*-factor = 2.0026) was also possible despite its irreversible character (Fig. 8d and e). In this case, the spin density is localized preferentially at the benzoisoindole moiety together with the acetylene-TIPS substituent (Fig. 8f). The promising results of these examples of π-extended ullazine derivatives open the door for the preparation of other systems with stronger OS characters and unique properties.

6. Conclusions and outlook

The search for materials with novel properties and enhanced performances plays a key role in the development of advanced real market technologies. Organic materials offer very appealing features compared to their inorganic counterparts such as easier fabrication processing, lightweight, possibility of deposition on a large variety of supports (rigid to flexible plastics to metal foils) and thin-film formation, for instance. (Het)-PAH-based materials have been widely studied and occupy a prominent place due to their rich molecular designs and unique properties. In this article, the most recent research studies on ullazine-based materials have been highlighted. While most of the N-doped PAH derivatives contain pyridinic-like nitrogen atoms, ullazine has at the central position of its π-conjugated system a pyrrolic nitrogen. As a consequence, an interesting intramolecular charge-separated character appears upon delocalisation of the lone pair of the nitrogen atom, which has been successfully exploited for the development of photosensitizers for solar energy conversion. Moreover, apart from allowing a fine-tuning of the electronic, optical and structural properties, the incorporation of nitrogen atoms into large conjugated systems indeed facilitates the formation of ionic and radical species. In this regard, the first examples of ullazine-based materials exhibiting challenging n-type charge-transport properties have been presented. Stable radical ions have been demonstrated as well, remarkably upon both oxidation and reduction.

However, although great attention has been paid so far to synthetic methodologies, proper characterisation studies of ullazine-based derivatives still remain scarce, and many questions concerning their potentialities are to be addressed in the near future. For instance, there are no studies concerning the impact of the disk-shaped structure along with its polarized π-system on the supramolecular arrangement, a critical parameter for the development of efficient organic semiconductors. Therefore, the door is wide open for future research works that will certainly uncover appealing features for the development of new (multi)-functional materials with improved performances for advanced applications, in particular in the field of organic electronics and solar energy harvesting.

Conflicts of interest

There are no conflicts to declare.

Acknowledgements

The author of this article is indebted to CNRS and the French Ministry of Research for financial support. The author would also like to thank Dr P. C. Gros, Dr S. Hesse and Dr P. Pierrat for fruitful collaborations. Dr Matteo Mauro is also acknowledged for valuable discussions.

Notes and references

1 M. Stępień, E. Gońka, M. Żyła and N. Sprutta, *Chem. Rev.*, 2016, **117**, 3479.
2 A. Narita, X.-Y. Wang, X. Feng and K. Müllen, *Chem. Soc. Rev.*, 2015, **44**, 6616.

3 W. Jiang, Y. Li and Z. Wang, *Chem. Soc. Rev.*, 2013, **42**, 6113.

4 A. L. Appleton, S. Miao, S. M. Brombosz, N. J. Berger, S. Barlow, S. R. Marder, B. M. Lawrence, K. I. Hardcastle and U. H. F. Bunz, *Org. Lett.*, 2009, **11**, 5222–5225.

5 S. More, R. Bhosale and A. Mateo-Alonso, *Chem. – Eur. J.*, 2014, **20**, 10626.

6 J. A. Schneider and D. F. Perepichka, *J. Mater. Chem. C*, 2016, **4**, 7269.

7 T. Miletić, A. Fermi, I. Orfanos, A. Avramopoulos, F. De Leo, N. Demitri, G. Bergamini, P. Ceroni, M. G. Papadopoulos, S. Couris and D. Bonifazi, *Chem. – Eur. J.*, 2017, **23**, 2363.

8 P. Hindenberg, A. López-Andarias, F. Rominger, A. de Cózar and C. Romero-Nieto, *Chem. – Eur. J.*, 2017, **23**, 13919.

9 X. Wang, G. Sun, P. Routh, D.-H. Kim, W. Huang and P. Chen, *Chem. Soc. Rev.*, 2014, **43**, 7067.

10 Q. Xiao, T. Sakurai, T. Fukino, K. Akaike, Y. Honsho, A. Saeki, S. Seki, K. Kato, M. Takata and T. Aida, *J. Am. Chem. Soc.*, 2013, **135**, 18268.

11 M. Kivala, W. Pisula, S. Wang, A. Mavrinskiy, J.-P. Gisselbrecht, X. Feng and K. Müllen, *Chem. – Eur. J.*, 2013, **19**, 8117.

12 B. He, A. B. Pun, L. M. Klivansky, A. M. McGough, Y. Ye, J. Zhu, J. Guo, S. J. Teat and Y. Liu, *Chem. Mater.*, 2014, **26**, 3920.

13 M. A. Squillaci, G. Markiewicz, A. Walczak, A. Ciesielski, A. R. Stefankiewicz and P. Samorì, *Chem. Commun.*, 2017, **53**, 9713.

14 S. Ito, Y. Tokimaru and K. Nozaki, *Angew. Chem., Int. Ed.*, 2015, **127**, 7364.

15 M. Takase, V. Enkelmann, D. Sebastiani, M. Baumgarten and K. Müllen, *Angew. Chem., Int. Ed.*, 2007, **46**, 5524.

16 A. L. Appleton, S. M. Brombosz, S. Barlow, J. S. Sears, J.-L. Brédas, S. R. Marder and U. H. F. Bunz, *Nat. Commun.*, 2010, **1**, 1.

17 U. H. F. Bunz, *Acc. Chem. Res.*, 2015, **48**, 1676.

18 J. Wei, B. Han, Q. Guo, X. Shi, W. Wang and N. Wei, *Angew. Chem., Int. Ed.*, 2010, **49**, 8209.

19 H. Li, F. S. Kim, G. Ren, E. C. Hollenbeck, S. Subramaniyan and S. A. Jenekhe, *Angew. Chem., Int. Ed.*, 2013, **52**, 5513.

20 A. Mateo-Alonso, *Chem. Soc. Rev.*, 2014, **43**, 6311.

21 R. Tang, F. Zhang, Y. Fu, Q. Xu, X. Wang, X. Zhuang, D. Wu, A. Giannakopoulos, D. Beljonne and X. Feng, *Org. Lett.*, 2014, **16**, 4726.

22 E. Gońka, P. J. Chmielewski, T. Lis and M. Stępień, *J. Am. Chem. Soc.*, 2014, **136**, 16399.

23 S. M. Draper, D. J. Gregg, E. R. Schofield, W. R. Browne, M. Duati, J. G. Vos and P. Passaniti, *J. Am. Chem. Soc.*, 2004, **126**, 8694.

24 H. Balli and M. Zeller, *Helv. Chim. Acta*, 1983, **66**, 2135.

25 V. Boekelheide and R. J. Windgassen, *J. Am. Chem. Soc.*, 1958, **80**, 2020.

26 F. Gerson and A. Metzger, *Helv. Chim. Acta*, 1983, **66**, 2031.

27 J. H. Delcamp, A. Yella, T. W. Holcombe, M. K. Nazeeruddin and M. Grätzel, *Angew. Chem., Int. Ed.*, 2013, **52**, 376.

28 A. Das, I. Ghosh and B. König, *Chem. Commun.*, 2016, **52**, 8695.

29 P. Pierrat, S. Hesse, C. Cebrián and P. C. Gros, *Org. Biomol. Chem.*, 2017, **15**, 8568.

30 D. Wan, X. Li, R. Jiang, B. Feng, J. Lan, R. Wang and J. You, *Org. Lett.*, 2016, **18**, 2876.

31 K.-I. Kanno, Y. Liu, A. Iesato, K. Nakajima and T. Takahashi, *Org. Lett.*, 2005, **7**, 5453.

32 N. A. Drigo, S. Paek, A. J. Huckaba, P. A. Schouwink, N. Tabet and M. K. Nazeeruddin, *Chem. – Eur. J.*, 2017, **23**, 17209.

33 D. Hou and H. Balli, *Helv. Chim. Acta*, 1992, **75**, 2608.

34 D. Ghorai and J. Choudhury, *ACS Catal.*, 2015, **5**, 2692.

35 Q. Ge, B. Li and B. Wang, *Org. Biomol. Chem.*, 2016, **14**, 1814.

36 D. L. Davies, C. E. Ellul, S. A. Macgregor, C. L. McMullin and K. Singh, *J. Am. Chem. Soc.*, 2015, **137**, 9659.

37 S. Boldt, S. Parpart, A. Villinger, P. Ehlers and P. Langer, *Angew. Chem., Int. Ed.*, 2017, **129**, 4646.

38 S. Parpart, S. Boldt, P. Ehlers and P. Langer, *Org. Lett.*, 2018, **20**, 122.

39 C. Li, Y. Liu, Z. Sun, J. Zhang, M. Liu, C. Zhang, Q. Zhang, H. Wang and X. Liu, *Org. Lett.*, 2018, **20**, 2806.

40 J.-I. Nishida, T. Fujita, Y. Fujisaki, S. Tokito and Y. Yamashita, *J. Mater. Chem.*, 2011, **21**, 16442.

41 S. Hashimoto, T. Ikuta, K. Shiren, S. Nakatsuka, J. Ni, M. Nakamura and T. Hatakeyama, *Chem. Mater.*, 2014, **26**, 6265–6271.

42 J. Dosso, J. Tasseroul, F. Fasano, D. Marinelli, N. Biot, A. Fermi and D. Bonifazi, *Angew. Chem., Int. Ed.*, 2017, **129**, 4554.

43 K. Matsui, S. Oda, K. Yoshiura, K. Nakajima, N. Yasuda and T. Hatakeyama, *J. Am. Chem. Soc.*, 2018, **140**, 1195.

44 J. Zhou, W. Yang, B. Wang and H. Ren, *Angew. Chem., Int. Ed.*, 2012, **51**, 12293.

45 R. Berger, A. Giannakopoulos, P. Ravat, M. Wagner, D. Beljonne, X. Feng and K. Müllen, *Angew. Chem., Int. Ed.*, 2014, **53**, 10520.

46 R. Berger, M. Wagner, X. Feng and K. Müllen, *Chem. Sci.*, 2015, **6**, 436.

47 S. Ito, Y. Tokimaru and K. Nozaki, *Chem. Commun.*, 2015, **51**, 221.

48 Y. Tokimaru, S. Ito and K. Nozaki, *Angew. Chem., Int. Ed.*, 2017, **56**, 15560.

49 A. Mishra, M. K. R. Fischer and P. Bäuerle, *Angew. Chem., Int. Ed.*, 2009, **48**, 2474.

50 A. Hagfeldt, G. Boschloo, L. Sun, L. Kloo and H. Pettersson, *Chem. Rev.*, 2010, **110**, 6595.

51 F. Bureš, *RSC Adv.*, 2014, **4**, 58826.

52 A. Dualeh, R. Humphry-Baker, J. H. Delcamp, M. K. Nazeeruddin and M. Grätzel, *Adv. Energy Mater.*, 2012, **3**, 496.

53 X. Jiang, K. M. Karlsson, E. Gabrielsson, E. M. J. Johansson, M. Quintana, M. Karlsson, L. Sun, G. Boschloo and A. Hagfeldt, *Adv. Funct. Mater.*, 2011, **21**, 2944.

54 H. Qiao, Y. Deng, R. Peng, R. Wang, J. Yuan and S. Tan, *RSC Adv.*, 2016, **6**, 70046.

55 S. Mathew, N. A. Astani, B. F. E. Curchod, J. H. Delcamp, M. Marszalek, J. Frey, U. Rothlisberger, M. K. Nazeeruddin and M. Grätzel, *J. Mater. Chem. A*, 2016, **4**, 2332.

56 C.-L. Wang, C.-M. Lan, S.-H. Hong, Y.-F. Wang, T.-Y. Pan, C.-W. Chang, H.-H. Kuo, M.-Y. Kuo, E. W.-G. Diau and C.-Y. Lin, *Energy Environ. Sci.*, 2012, **5**, 6933.

57 A. Facchetti, *Mater. Today*, 2007, **10**, 28.

58 W. Wu, Y. Liu and D. Zhu, *Chem. Soc. Rev.*, 2010, **39**, 1489.

59 C. Wang, H. Dong, W. Hu, Y. Liu and D. Zhu, *Chem. Rev.*, 2012, **112**, 2208.

60 L. Zhang, Y. Cao, N. S. Colella, Y. Liang, J.-L. Brédas, K. N. Houk and A. L. Briseno, *Acc. Chem. Res.*, 2015, **48**, 500.

61 X. Cui, C. Xiao, L. Zhang, Y. Li and Z. Wang, *Chem. Commun.*, 2016, **52**, 13209.

62 H. Tsuji and E. Nakamura, *Acc. Chem. Res.*, 2017, **50**, 396.

63 J. Feng, W. Jiang and Z. Wang, *Chem. – Asian J.*, 2017, **13**, 20.

64 G. H. Gelinck, H. E. A. Huitema, E. van Veenendaal, E. Cantatore, L. Schrijnemakers, J. B. P. H. van der Putten, T. C. T. Geuns, M. Beenhakkers, J. B. Giesbers, B.-H. Huisman, E. J. Meijer, E. M. Benito, F. J. Touwslager, A. W. Marsman, B. J. E. van Rens and D. M. de Leeuw, *Nat. Mater.*, 2004, **3**, 106.

65 J. Y. Oh, S. Rondeau-Gagné, Y.-C. Chiu, A. Chortos, F. Lissel, G.-J. N. Wang, B. C. Schroeder, T. Kurosawa, J. Lopez, T. Katsumata, J. Xu, C. Zhu, X. Gu, W.-G. Bae, Y. Kim, L. Jin, J. W. Chung, J. B. H. Tok and Z. Bao, *Nature*, 2016, **539**, 411–415.

66 M. Kaltenbrunner, T. Sekitani, J. Reeder, T. Yokota, K. Kuribara, T. Tokuhara, M. Drack, R. Schwödiauer, I. Graz, S. Bauer-Gogonea, S. Bauer and T. Someya, *Nature*, 2013, **499**, 458.

67 B. Comiskey, J. D. Albert, H. Yoshizawa and J. Jacobson, *Nature*, 1998, **394**, 253.

68 H. Dong, X. Fu, J. Liu, Z. Wang and W. Hu, *Adv. Mater.*, 2013, **25**, 6158.

69 X. Gao and Y. Hu, *J. Mater. Chem. C*, 2014, **2**, 3099.

70 A. Skabeev, U. Zschieschang, Y. Zagranyarski, H. Klauk, K. Müllen and C. Li, *Org. Lett.*, 2018, **20**, 1409.

71 J. Roncali, *Chem. Rev.*, 1997, **97**, 173.

72 M. Bendikov, F. Wudl and D. F. Perepichka, *Chem. Rev.*, 2004, **104**, 4891.

73 J. E. Anthony, *Chem. Rev.*, 2006, **106**, 5028.

74 T. Weil, T. Vosch, J. Hofkens, K. Peneva and K. Müllen, *Angew. Chem., Int. Ed.*, 2010, **49**, 9068.

75 M. Bendikov, H. M. Duong, K. Starkey, K. N. Houk, E. A. Carter and F. Wudl, *J. Am. Chem. Soc.*, 2004, **126**, 7416.

76 G. D. Scholes and G. Rumbles, *Nat. Mater.*, 2006, **5**, 683.

77 M. Pinheiro, L. F. A. Ferrão, F. Bettanin, A. J. A. Aquino, F. B. C. Machado and H. Lischka, *Phys. Chem. Chem. Phys.*, 2017, **19**, 19225.

78 A. Konishi, Y. Hirao, M. Nakano, A. Shimizu, E. Botek, B. Champagne, D. Shiomi, K. Sato, T. Takui, K. Matsumoto, H. Kurata and T. Kubo, *J. Am. Chem. Soc.*, 2010, **132**, 11021.

79 Z. Sun and J. Wu, *J. Mater. Chem.*, 2012, **22**, 4151.

80 Z. Zeng, X. Shi, C. Chi, J. T. López Navarrete, J. Casado and J. Wu, *Chem. Soc. Rev.*, 2015, **44**, 6578.

81 K. Kamada, K. Ohta, T. Kubo, A. Shimizu, Y. Morita, K. Nakasuji, R. Kishi, S. Ohta, S.-I. Furukawa, H. Takahashi and M. Nakano, *Angew. Chem., Int. Ed.*, 2007, **46**, 3544.

82 M. Nakano and B. Champagne, *J. Phys. Chem. Lett.*, 2015, **6**, 3236.

83 Y. Morita, S. Nishida, T. Murata, M. Moriguchi, A. Ueda, M. Satoh, K. Arifuku, K. Sato and T. Takui, *Nat. Mater.*, 2011, **10**, 947.

84 Y. Morita, S. Suzuki, K. Sato and T. Takui, *Nat. Chem.*, 2011, **3**, 197.

85 O. Anamimoghadam, M. D. Symes, D.-L. Long, S. Sproules, L. Cronin and G. Bucher, *J. Am. Chem. Soc.*, 2015, **137**, 14944.

86 M. Richter, K. S. Schellhammer, P. Machata, G. Cuniberti, A. Popov, F. Ortmann, R. Berger, K. Müllen and X. Feng, *Org. Chem. Front.*, 2017, **4**, 847.